

Double explosive transition in the synchronization of multilayer networks

Tianwei Wu,¹ Siyu Huo,¹ K. Alfaro-Bittner,² S. Boccaletti,^{2,3,4,*} and Zonghua Liu^{1,†}

¹State Key Laboratory of Precision Spectroscopy and School of Physics and Electronic Science, East China Normal University, Shanghai 200241, People's Republic of China

²Universidad Rey Juan Carlos, Calle Tulipán s/n, 28933 Móstoles, Madrid, Spain

³CNR - Institute of Complex Systems, Via Madonna del Piano 10, I-50019 Sesto Fiorentino, Italy

⁴Moscow Institute of Physics and Technology, Dolgoprudny, Moscow Region 141701, Russian Federation



(Received 12 January 2022; accepted 16 June 2022; published 5 July 2022)

We give evidence that consecutive explosive transitions may occur in two-layered networks, when a dynamical layer made of an ensemble of networking phase oscillators interacts with an environmental layer of oscillators which are in a state of approximate synchronization. Under these conditions, the interlayer coupling induces two consecutive explosive transitions in the dynamical layer, each one associated with a hysteresis loop. We also show that the same phenomenon can be observed when the environmental layer is simplified into a single node with phase lag. Theoretical arguments unveil that the mechanisms at the basis of the two transitions are in fact different, with the former originating from a coupling-amplified disorder and the latter originating from a coupling-induced synchronization. We discuss the relevance of the observed state in brain dynamics and show how it may emerge in a real brain network.

DOI: [10.1103/PhysRevResearch.4.033009](https://doi.org/10.1103/PhysRevResearch.4.033009)

Explosive synchronization (ES) [1] refers to the appearance (or disappearance) of synchronization in a system following a first-order-like phase transition, i.e., a scenario where order (or disorder) sets in within the system in an abrupt, discontinuous way. In some cases, ES has an irreversible character and is accompanied by a hysteresis loop when the control parameter undergoes forward and backward adiabatic processes [2]. Different mechanisms have been revealed as possible ways leading to ES [3–26]: (i) the combination of heterogeneity in the network's degree distribution and a positive correlation between the natural frequencies of the oscillatory units and their degrees [3–5] (conditions that have been later extended to the cases of partial frequency-degree correlation [18,19] and frequency-weighted networks [8,20]); (ii) a frequency-weighted coupling strength [6]; (iii) a locally adaptive coupling in mono- and multilayer networks [12–17]; and (iv) the addition of quenched disorder to the oscillators' frequencies [11,27], or the simultaneous presence of cooperation [28] or percolation [29], or even the presence of time delay [21–23]. It was later shown that all these scenarios can be actually seen as different realizations of a suppressive rule for pairwise synchronization [9], i.e., a frustration mechanism which contrasts the formation or growth of small clusters of synchronized oscillators at intermediate coupling strengths. Recently, explosive transitions have been shown to be a

universal feature of nonlinear dynamical systems that have a generic two-parameter family [30].

So far, studies have concentrated on networked systems displaying a single ES transition when progressively increasing (or decreasing) the coupling strength, accompanied by either no hysteresis loop or only one hysteresis loop [31]. Then, the question arises as to whether multiple, consecutive, explosive transitions can be observed in a single system. This issue is relevant, for instance, in brain dynamics, where neural synchronization is commonly found during the execution of a number of tasks [32,33]. Then, a group of neurons which has to pass from performing a task to operating on another one needs in fact to experience an abrupt desynchronization from the ordered state associated with the accomplishment of the first task followed by an equally abrupt synchronization to the different ordered state associated with the new task.

In this paper, we give evidence that consecutive explosive transitions take place in a multilayer network, each one associated with its own hysteresis loop. Precisely, we consider a two-layered network, with one layer accounting for a sort of environmental system featuring approximate synchronization and the other layer describing instead the networked dynamical system under study. In these conditions, the interlayer coupling induces two consecutive explosive transitions in the dynamical layer. We further show that the same phenomenon can be observed also when simplifying the environmental layer into a single node with phase lag. By theoretical analysis we demonstrate that the mechanisms at the basis of the two transitions are in fact different, with the former originating from a coupling-amplified disorder and the latter originating from a coupling-induced synchronization. Finally, we prove that the state discussed here can actually emerge in a real brain network.

*stefano.boccaletti@gmail.com

†zhliu@phy.ecnu.edu.cn

Published by the American Physical Society under the terms of the [Creative Commons Attribution 4.0 International](https://creativecommons.org/licenses/by/4.0/) license. Further distribution of this work must maintain attribution to the author(s) and the published article's title, journal citation, and DOI.

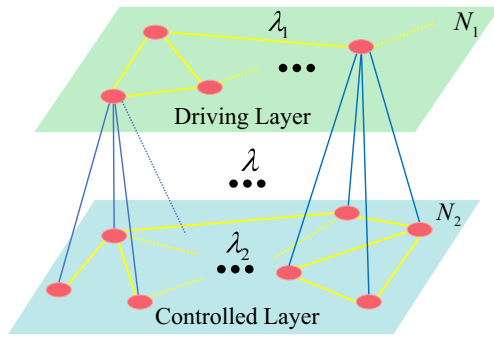


FIG. 1. Sketch of a two-layered network, with the first layer being the environmental layer and the second one being the dynamical layer.

Let us start by considering a two-layered network, such as the one sketched in Fig. 1, where the first (or upper) layer represents an environmental system and the second (or lower) layer represents instead a generic networked dynamical system. In what follows (and unless otherwise specified) the two layers are independent random Erdős-Rényi (ER) networks [34], with N_1 and N_2 nodes and average degrees $\langle k_1 \rangle$ and $\langle k_2 \rangle$, respectively. Moreover, in Fig. 1 and in the rest of this paper, we denote by λ_1 and λ_2 the intralayer coupling strength of the first and second layer, respectively, while we denote by λ the interlayer coupling strength. For simplicity, we here only consider the case of $N_1 = N_2 \equiv N$, in which furthermore each node is represented by a Kuramoto phase oscillator [35].

Considering that the synchronization of two-layered networks has been well studied for the case of the same intra- and intercouplings, it is maybe necessary for us to consider a few specific cases where some interesting results can be expected. One such paradigmatic example is the finding of explosive synchronization, which comes from the specific conditions of both a scale-free network and a positive correlation between the natural frequencies and nodes' degrees [3], in contrast to the general discussions based on the analysis of the master stability function. In this sense, we here consider a specific situation where all oscillators of the network are influenced by almost the same environmental signal. In the setup of Fig. 1, this is realized by letting the natural frequencies of each environmental oscillator be slightly different to prohibit complete synchronization, and yet considering always a value of λ_1 which is large enough to determine approximate synchronization. Moreover, we will consider the case in which the two layers display considerably different frequency distributions, with the environmental (dynamical) layer being made of low-frequency (high-frequency) oscillators. The resulting dynamics can be described by

$$\begin{aligned} \dot{\theta}_{i,1} &= \omega_{i,1} + \lambda_1 \sum_{j=1}^N A_{ij,1} \sin(\theta_{j,1} - \theta_{i,1}) + \lambda \sin(\theta_{i,2} - \theta_{i,1}), \\ \dot{\theta}_{i,2} &= \omega_{i,2} + \lambda_2 \sum_{j=1}^N A_{ij,2} \sin(\theta_{j,2} - \theta_{i,2}) + \lambda \sin(\theta_{i,1} - \theta_{i,2}), \end{aligned} \tag{1}$$

where $i = 1, 2, \dots, N$, the subscripts 1 and 2 stand for the upper and lower layer, respectively, and $\omega_{i,1}$ and $\omega_{i,2}$ denote the natural frequencies of the nonidentical oscillators in the first and second layer, respectively. A_{ij} are the elements of the adjacency matrix A (with $A_{ij} = 1$ if nodes i and j of the same layer are connected, and $A_{ij} = 0$ otherwise). Finally, the last term on the right-hand side of Eqs. (1) accounts for the interlayer coupling.

In order to better illustrate the observed phenomenon, we here set the frequencies in the environmental layer (in the network) to be equispaced and homogeneously distributed around a central frequency ω_0 ($3\omega_0$). Precisely, we set $\omega_{i,1} = \omega_i + \omega_0$ and $\omega_{i,2} = \omega_i + 3\omega_0$, with $\omega_i = \pi \Delta(2i - (N - 1))/2(N - 1)$. Furthermore, we fix $\langle k_1 \rangle = \langle k_2 \rangle = 10$, $\omega_0 = 3.0$, and $N = 200$, and we study how the interlayer coupling strength λ drives the synchronization transition in the network layer. This is monitored by the global order parameters R_1 and R_2 of the first and second layer, defined by $R_1 e^{i\psi_1} = \frac{1}{N_1} \sum_{j=1}^{N_1} e^{i\theta_{j,1}}$ and $R_2 e^{i\psi_2} = \frac{1}{N_2} \sum_{j=1}^{N_2} e^{i\theta_{j,2}}$. Specifically, we denote with R_{1F} and R_{1B} (R_{2F} and R_{2B}) the values of R_1 (R_2) obtained during the forward and backward synchronization processes. Moreover, we introduce the effective frequency $\omega_{i,2}^{\text{eff}} = \frac{1}{T} \int_t^{t+T} \dot{\theta}_{i,2}(\tau) d\tau$ for the second layer, with $T \gg 1$, and denote by ω_{2F} and ω_{2B} the values of $\omega_{i,2}^{\text{eff}}$ measured during the forward and backward processes. Similarly, $\omega_{i,1}^{\text{eff}}$, ω_{1F} , and ω_{1B} are introduced.

In our simulations, initial phases of all oscillators are drawn from a random uniform distribution in the range $[0, 2\pi)$. In order to simulate the forward (backward) process, λ is then adiabatically increased (decreased) from $\lambda = 0$ to $\lambda = 5$ (from $\lambda = 5$ to $\lambda = 0$) with increment (decrement) of $\delta\lambda = 0.02$ at each step [36], and the order parameters R_{1F} and R_{2F} (R_{1B} and R_{2B}) are calculated for each λ .

When the parameter Δ is sufficiently large, Eqs. (1) give rise to a classical scenario of ES transition. However, a phenomenon is featured by the network layer for relatively small Δ : Starting from the state where both layers are synchronized (though at different frequencies), the network layer experiences two consecutive explosive transitions, the first corresponding to an abrupt desynchronization and the second corresponding to an explosive resynchronization.

The results are reported in Figs. 2(a) and 2(b), which display R_2 vs λ for $\Delta = 0.001$, $\lambda_1 = 2.4$, and $\lambda_2 = 0.02$ [Fig. 2(a)] and the corresponding values of $\omega_{i,2}^{\text{eff}}$ and $\omega_{i,1}^{\text{eff}}$ [Fig. 2(b)]. Figure 2(a) reveals that R_2 features two consecutive explosive transitions (each one associated with a hysteresis loop), while R_1 does not, confirming that the environmental layer remains approximately synchronized. Figure 2(b) reveals that $\omega_{i,2}^{\text{eff}}$ decreases with the increase in the interlayer coupling strength λ and eventually reaches a value of $2\omega_0$ when the two layers are synchronized. $\omega_{i,2}^{\text{eff}}$ shows also two small loops in correspondence with the hysteresis loops of R_2 .

Do the results of Figs. 2(a) and 2(b) depend on the distributions of the natural frequencies $\omega_{i,1}$ and $\omega_{i,2}$? To check this, we have made simulations on other distributions and found similar observations. The reason is that the range of the natural frequencies is chosen as $\pi \Delta$, which is very small when $\Delta = 0.001$. Thus different distributions do not make a

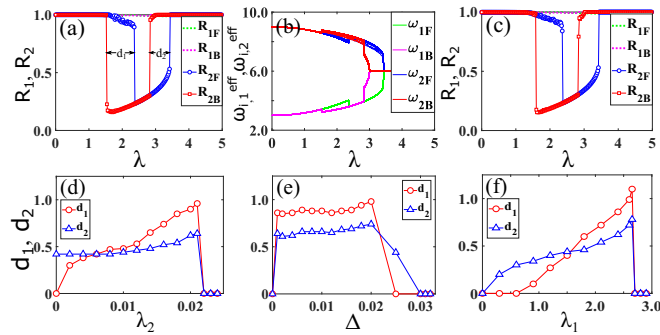


FIG. 2. (a) The two consecutive explosive transitions featured by the dynamical layer. $\lambda_1 = 2.4$ and $\lambda_2 = 0.02$ (other parameters specified in the text). The blue line with circles (red line with squares) indicates the R_2 values during the forward (backward) transition. The forward and backward R_1 values are also reported as dashed lines. (b) $\omega_{i,2}^{\text{eff}}$ and $\omega_{i,1}^{\text{eff}}$ (see text for definition) vs λ , in the same conditions as in (a). (c) The case of Gaussian distribution with other parameters being the same as in (a). (d), (e), and (f) The widths d_1 and d_2 of the two hysteresis loops vs the parameters λ_2 , Δ , and λ_1 , respectively, with the other parameters being fixed as $\lambda_1 = 2.4$ and $\Delta = 0.001$ in (d), $\lambda_1 = 2.4$ and $\lambda_2 = 0.02$ in (e), and $\Delta = 0.001$ and $\lambda_2 = 0.02$ in (f).

large difference among individual $\omega_{i,1}$ and $\omega_{i,2}$, resulting in a robustness to the frequency distribution. As an example, Fig. 2(c) shows the results on a Gaussian distribution with mean $\langle \omega_i \rangle = 0$ and variance $\sigma = 0.0009$ ($\approx \Delta$) and with other parameters unchanged. We see that it is almost the same as Fig. 2(a). Therefore we will only focus on the case of Fig. 2(a) in the following discussions.

Next, we denote by d_1 and d_2 the widths of the first and second hysteresis loops and study their dependence on the parameters λ_2 , Δ , and λ_1 . The results are shown in Figs. 2(d)–2(f). Figure 2(d) reveals that the two hysteresis loops exist in a small range of λ_2 (0, 0.021). When $\lambda_2 = 0.022$, the two loops merge and disappear simultaneously. Figure 2(e) indicates that the two loops exist only for $\Delta < 0.025$. This is a relatively narrow range, and its limited extension is mainly determined by the need to maintain the controlled layer in its synchronous state. Figure S1 in the Supplemental Material (SM) [37] shows, instead, that similar scenarios can be obtained for larger frequency ranges in the upper layer. Figure 2(f) reveals that the two hysteresis loops exist in the range $0.6 < \lambda_1 < 2.7$, i.e., for a condition of large enough intracoupling within the environmental layer, which is responsible for keeping it almost synchronized during the entire process of the double transition occurring in the lower layer.

The fact that the environmental layer always stays in a state of approximate synchronization allows one to simplify the study, by reducing the first layer to a single environmental node. Figure 3 shows a sketch of such a network.

Considering that the oscillators are nonidentical with distributed frequencies, complete synchronization is impossible, and thus the coupling between the two layers of Eqs. (1) is slightly different from one interlink to another. In this sense, one can safely assume that the small fluctuations from perfect synchronization can be accounted for by a phase lag τ_i [38],

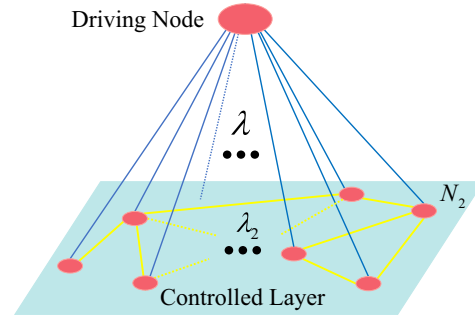


FIG. 3. Sketch of a network coupled to a single node, by reducing the first layer of Fig. 1 to a single environmental node.

so that Eqs. (1) are now rewritten as ($i = 1, 2, \dots, N$)

$$\begin{aligned} \dot{\theta}_1 &= \omega_1 + \frac{\lambda}{N} \sum_{j=1}^N \sin(\theta_{j,2} - \theta_1 - \tau_j), \\ \dot{\theta}_{i,2} &= \omega_{i,2} + \lambda_2 \sum_{j=1}^N A_{ij,2} \sin(\theta_{j,2} - \theta_{i,2}) \\ &\quad + \lambda \sin(\theta_1 - \theta_{i,2} - \tau_i). \end{aligned} \tag{2}$$

The case of an identical phase lag ($\tau_i = \tau = 0.2$) is reported in Fig. 4(a), which shows that once again two consecutive explosive transitions are featured by the networked system. Figures 4(c) and 4(d) report the widths d_1 and d_2 or the hysteresis loops associated with the two transitions vs λ_2 and τ , respectively, with $\tau = 0.05$ in Fig. 4(c) and $\lambda_2 = 0.02$ in Fig. 4(d). From Fig. 4(c) one sees that the loops disappear when $\lambda_2 > 0.021$, while Fig. 4(d) shows that they exist in

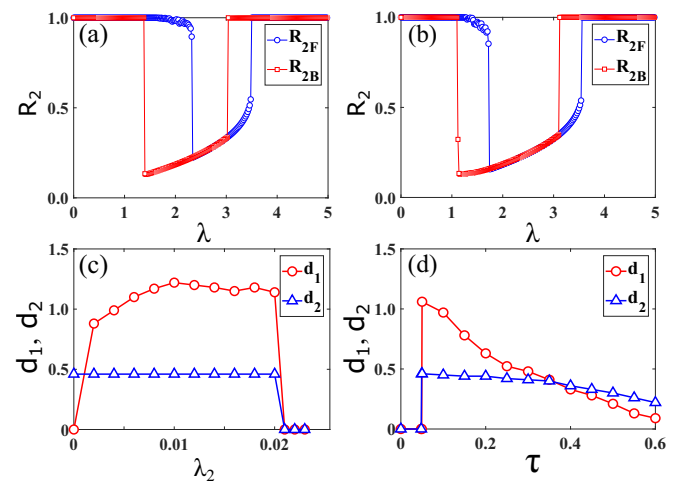


FIG. 4. The two consecutive explosive transitions for the case of a single environmental node, described in Eqs. (2), with $N = 200$, $\langle k_2 \rangle = 10$, and $\Delta = 0.001$. (a) and (b) report R_2 for the cases of identical ($\tau = 0.2$) and distributed [$\tau_i \in (0, 0.1)$] phase lag, respectively. $\lambda_2 = 0.02$ in (a) and $\lambda_2 = 0.005$ in (b). The blue line with circles (red line with squares) indicates the R_2 values during the forward (backward) transition. (c) and (d) show the hysteresis widths d_1 and d_2 vs the parameters λ_2 and τ , respectively, in the case of identical phase lag $\tau = 0.05$ in (c) and $\lambda_2 = 0.02$ in (d).

the range $0.05 < \tau < 0.6$, i.e., the two hysteresis loops are induced in specific ranges of λ_2 and τ .

Then, we move to consider the case of distributed time delays, i.e., different τ_i for different nodes in the networked system, and randomly draw τ_i from a homogeneous distribution. Figure 4(b) shows the results for $\tau_i \in (0, 0.1)$ and $\lambda_2 = 0.005$, which once again clearly shows the presence of two consecutive explosive transitions.

At this stage, it is worth discussing few points in support of the observed scenario, while the interested reader can find a much more detailed theoretical description in the SM [37]. The main conclusion which can be drawn from our results is that the two explosive transitions are induced in fact by two different mechanisms. In particular, the first is coming from the fact that the intercoupling actually amplifies the small differences among the oscillators of the dynamical layer inducing a dynamical instability. In other words, the intercoupling term acts as a disturbance whose strength is increasing with λ . Once it is strong enough to counter the weak intracoupling term, synchronization of the dynamical layer is broken. To illustrate this argument, we take a simplified approach, where the environmental layer is seen as a single node and the dynamical layer reduces to two coupled nodes with frequency mismatch Δ . In this case, Eqs. (2) reduce to

$$\begin{aligned}\dot{\theta}_1 &= \omega_1 + \frac{\lambda}{2} [\sin(\theta_2 - \theta_1 - \tau_1) + \sin(\theta_3 - \theta_1 - \tau_2)], \\ \dot{\theta}_2 &= \omega_2 + \lambda_2 \sin(\theta_3 - \theta_2) + \lambda \sin(\theta_1 - \theta_2 - \tau_1), \\ \dot{\theta}_3 &= \omega_3 + \lambda_2 \sin(\theta_2 - \theta_3) + \lambda \sin(\theta_1 - \theta_3 - \tau_2),\end{aligned}\quad (3)$$

with $\omega_1 = \omega_0$, $\omega_2 = 3\omega_0$, and $\omega_3 = \omega_2 + \Delta$. Letting $\delta\theta = \theta_3 - \theta_2$, one has

$$\begin{aligned}\delta\dot{\theta} &= \Delta - 2\lambda_2 \sin(\delta\theta) + \lambda [\sin(\theta_1 - \theta_3 - \tau_2) \\ &\quad - \sin(\theta_1 - \theta_2 - \tau_1)].\end{aligned}\quad (4)$$

Specifically, when $\tau_2 = \tau_1 + \pi$, we have

$$\begin{aligned}\delta\dot{\theta} &= \Delta - 2\lambda_2 \sin(\delta\theta) - \lambda [\sin(\theta_1 - \theta_3 - \tau_1) \\ &\quad + \sin(\theta_1 - \theta_2 - \tau_1)].\end{aligned}\quad (5)$$

When $\delta\theta \ll 1$, one has $\sin(\delta\theta) \approx 0$ and $\theta_3 \approx \theta_2$, and thus

$$\delta\dot{\theta} = \Delta - 2\lambda \sin(\theta_1 - \theta_2 - \tau_1).\quad (6)$$

As there is a big difference between $\omega_1 = \omega_0 = 3.0$ and $\omega_2 = 3\omega_0 = 9.0$, the term $\sin(\theta_1 - \theta_2 - \tau_1)$ in Eq. (6) will change periodically with time t , i.e., being positive half the time and negative half the time. Thus the right-hand side of Eq. (6) will be positive for more than half of a period, as $\Delta > 0$. In this sense, $\delta\theta$ will not approach zero but will increase with time t , indicating that the synchronization solution of $\delta\theta = 0$ of the dynamical layer will lose its stability. To confirm this theoretical analysis, Figs. 5(a) and 5(b) show the corresponding numerical simulations with $\omega_1 = 3.0$, $\omega_2 = 9.0$, $\omega_3 = 9.0 + \Delta$, $\Delta = 0.001$, $\lambda_2 = 0.02$, and $\tau_2 = \tau_1 + \pi$, where Figs. 5(a) and 5(b) represent the cases of $\tau_1 = 0.1$ and 0.2 , respectively. We see that they do have explosive transitions, thus explaining the mechanism of the first hysteresis loop in Figs. 2 and 4.

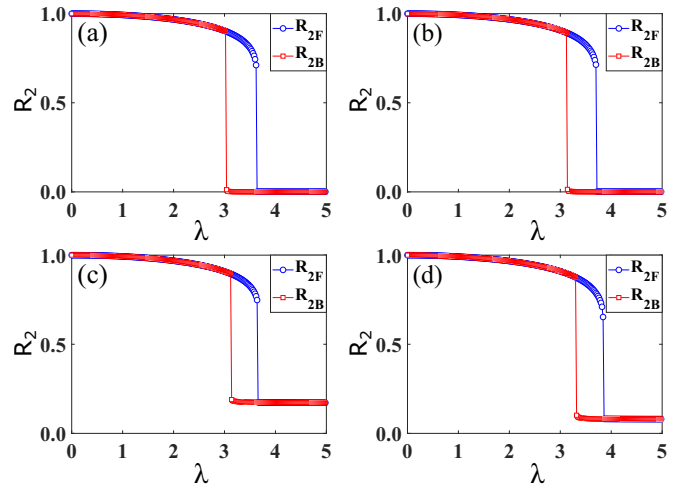


FIG. 5. The explosive transition for the case of three oscillators with the first one as a single environmental node and the other two as the dynamical layer, described in Eqs. (3), with $\omega_1 = 3.0$, $\omega_2 = 9.0$, $\omega_3 = 9.0 + \Delta$, $\Delta = 0.001$, and $\lambda_2 = 0.02$. (a) and (b) represent the case of $\tau_2 = \tau_1 + \pi$, with $\tau_1 = 0.1$ in (a) and $\tau_1 = 0.2$ in (b). (c) and (d) represent the case of $\tau_2 \neq \tau_1 + \pi$, with $\tau_1 = 0.2$ and $\tau_2 = \tau_1 + 2.8 = 3.0$ in (c) and $\tau_2 = \tau_1 + 3.3 = 3.5$ in (d). The blue line with circles (red line with squares) indicates the R_2 values during the forward (backward) transition.

Notice that Eq. (6) is based on the condition $\tau_2 = \tau_1 + \pi$, which makes the coupling term $\lambda [\sin(\theta_1 - \theta_3 - \tau_2) - \sin(\theta_1 - \theta_2 - \tau_1)]$ in Eq. (4) be maximum. However, even when the condition is not satisfied, it is still possible to make the right-hand side of Eq. (4) be positive in part of the period and, consequently, to make the synchronized solution $\delta\theta = 0$ unstable. Figures 5(c) and 5(d) show the numerical simulations with $\tau_1 = 0.2$ and $\tau_2 \neq \tau_1 + \pi$, where Figs. 5(c) and 5(d) represent the cases of $\tau_2 = \tau_1 + 2.8 = 3.0$ and $\tau_2 = \tau_1 + 3.3 = 3.5$, respectively. We see that the hysteresis loops in Figs. 5(c) and 5(d) are smaller than those in Figs. 5(a) and 5(b), thus confirming our theoretical analysis. On the other hand, one sees that the differences between values of τ_i in Figs. 4(a) and 4(b) are much smaller than the difference $(\tau_2 - \tau_1) \sim \pi$ in Eq. (5). The reason is that there is a large number of oscillators in Figs. 4(a) and 4(b) and their accumulated influence on a node will be large, i.e., equivalent to that of $(\tau_2 - \tau_1) \sim \pi$ in Eq. (5).

Finally, we give evidence that the described phenomenon is in fact helpful for us to characterize the dynamics and functioning of a real brain network. It is known that brain networks can be separated into different cognitive subnetworks and thus naturally form a multilayered network structure [39], where layers correspond to the frequency bands at which the brain operates [40]. Such a layered structure has been confirmed by magnetoencephalographic recordings [41,42]. Now, when a specific input signal is received by a brain network at the rest state, the network is switched from the rest state to the task state, and the corresponding cognitive subnetwork is activated while others remain inactive [43]. Such an explosive transition may be compared with the first hysteresis loop in our two-transition model, while the second hysteresis loop

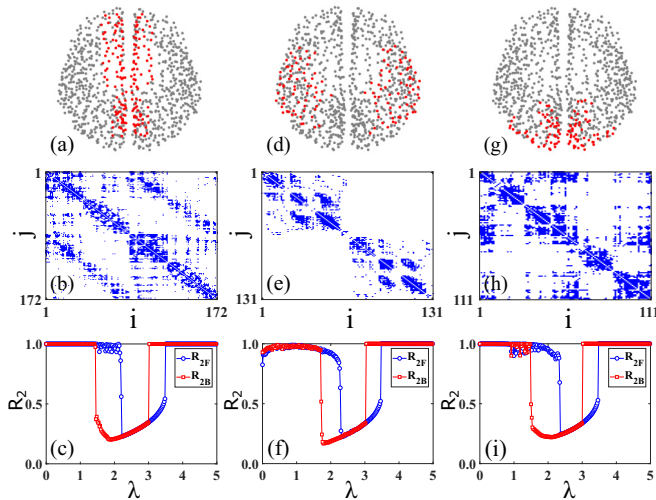


FIG. 6. Multiple explosive transitions occurring on the medial default mode, ventral temporal association, and visual subnetworks. The first, second, and third rows display the location of the nodes (red dots) on the brain network, the connection matrix, and R_2 vs λ , respectively. (a)–(c) represent the case of the medial default mode subnetwork with $N = 172$, $\langle k \rangle \approx 29.56$, $\lambda_2 = 0.01$, $\Delta = 0.001$, and $\tau = 0.06$. (d)–(f) represent the case of the ventral temporal association subnetwork with $N = 129$, $\langle k \rangle \approx 12.63$, $\lambda_2 = 0.01$, $\Delta = 0.001$, and $\tau = 0.08$. (g)–(i) represent the case of the visual subnetwork with $N = 111$, $\langle k \rangle \approx 22.99$, $\lambda_2 = 0.01$, $\Delta = 0.001$, and $\tau = 0.06$.

(the one occurring at larger coupling strengths) may be associated with the further switching from one dynamical state of the brain to another. This, in particular, shares similarities with what seems to happen at the onset of anesthetic-induced unconsciousness, where the inhaled anesthetic sevoflurane is used to gradually modulate the level of consciousness across multiple states, i.e., eyes-closed waking, unconsciousness, and recovery, and an abrupt state transition is observed [44].

We here take the network extracted from the brain data of Refs. [45,46]. In the data, the cerebral cortex is divided into 989 relatively uniform regions of interest (ROIs), with each representing a network node, and the connections within all possible pairs of the 989 ROIs were measured noninvasively by using diffusion spectrum imaging (DSI). According to the classification of cognitive subnetworks given in Ref. [47], one can partition the 989 nodes into eight cognitive subnetworks: attention, auditory, cingulo-opercular, frontoparietal, medial default mode, motor and somatosensory, ventral temporal association, and visual subnetworks. When performance of a specific cognitive task is needed, the corresponding subnetwork is activated, while all the other seven subnetworks remain inactive. Therefore the activated cognitive subnetwork is taken as the dynamical layer, and all the other subnetworks form the environmental layer. Furthermore, we simplify the environmental layer as a single environmental node, and we simulate Eqs. (2) at a fixed value of τ .

For the medial default mode subnetwork, Fig. 6(a) shows the position of nodes in the brain network; they are distributed along the middle part, i.e., the corpus callosum, and thus have a dense structure of intralinks. Figure 6(b)

shows its connection matrix, displaying a modular topology with a high number of interlinks among communities. Figure 6(c) shows the order parameter of the dynamical layer R_2 for $\tau = 0.06$, where the blue line with circles (red line with squares) represents the forward (backward) processes of R_2 . It is easy to see that with the increase in the intercoupling strength λ , the subnetwork displays two consecutive ES transitions.

The same simulations are performed for the case of the ventral temporal association subnetwork, which is now located away from the middle region of the brain [see Fig. 6(d)] and is divided into three communities, with a small one at the middle and the other two big ones at the upper left and lower right, respectively, with a negligible number of interlinks among the three communities, indicating that they are almost isolated [see Fig. 6(e)]. Figure 6(f) shows that, once again, multiple explosive transition occur in such a topological arrangement. Finally, we consider the case of the visual subnetwork. Figure 6(g) shows that, at variance with the previous two cases, the subnetwork nodes are now located in the bottom region of the brain. From Fig. 6(h), one can see that the subnetwork displays again a modular structure, characterized, however, by a density of interlinks which stays in between the previous two cases. Once again, Fig. 6(i) reveals the occurrence of multiple ES transitions.

Far from being limited to brain dynamics, we would like to remark that the same phenomenon is expected to occur also in other networked systems, provided that they have the structure of Fig. 1 and they satisfy the conditions discussed in this paper. For instance, it is well known that, together with primary cascading failures, power grids may also suffer secondary cascading failures in local parts of the network, i.e., secondary disasters [48]. Moreover, similar phenomena are known to occur in epidemic spreading, when recurrent epidemics may break out from time to time [49–52].

In conclusion, we have given evidence that a two-layered network may experience consecutive ES transitions. The phenomenon occurs in a dynamical layer subject to interaction with an environmental layer which always operates in a regime of approximate synchronization. At variance with previous studies on ES, the cascade of two explosive transitions is here induced by increasing the coupling strength between the two layers. Moreover, we have shown that the two explosive transitions are accompanied by two distinct hysteresis loops, and we have reported how the widths of such loops depend on the fundamental parameters of the model. With theoretical arguments we have further shown that the first hysteresis loop comes from a coupling-amplified disorder mechanism, while the second one is similar to the classical case of coupling-induced synchronization. Finally, we have shown that the same scenario can be observed when the environmental layer is simplified into a single node with phase lag, and we have proven that consecutive ES transitions can indeed emerge in a real brain network. Our results disclose the option for an explosive desynchronization-resynchronization transition mechanism and are of value, for instance, in brain dynamics, to describe a possible way in which a group of neurons can switch from performing one task to

operating on another one, i.e., an abrupt desynchronization from the ordered state associated with the accomplishment of the first task followed by an equally abrupt synchronization to the different ordered state associated with the new task.

This work was partially supported by the “Technology Innovation 2030 Major Projects” on brain science and brain-like computing of the MST of China (No. 2021ZD0202600) and the NNSF of China under Grants No. 11835003, No. 82161148012, and No. 12175070.

-
- [1] S. Boccaletti, J. A. Almendral, S. Guan, I. Leyva, Z. Liu, I. Sendiña-Nadal, Z. Wang, and Y. Zou, Explosive transitions in complex networks’ structure and dynamics: Percolation and synchronization, *Phys. Rep.* **660**, 1 (2016).
- [2] H. Sakaguchi, Synchronization in coupled phase oscillators, *J. Korean Phys. Soc.* **53**, 1257 (2008).
- [3] J. Gómez-Gardeñes, S. Gómez, A. Arenas, and Y. Moreno, Explosive Synchronization Transitions in Scale-Free Networks, *Phys. Rev. Lett.* **106**, 128701 (2011).
- [4] I. Leyva, R. Sevilla-Escoboza, J. M. Buldú, I. Sendiña-Nadal, J. Gomez-Gardeñes, A. Arenas, Y. Moreno, S. Gómez, R. Jaimes-Reátegui, and S. Boccaletti, Explosive First-Order Transition to Synchrony in Networked Chaotic Oscillators, *Phys. Rev. Lett.* **108**, 168702 (2012).
- [5] P. Kundu, P. Khanra, C. Hens, and P. Pal, Transition to synchrony in degree-frequency correlated Sakaguchi-Kuramoto model, *Phys. Rev. E* **96**, 052216 (2017).
- [6] X. Zhang, X. Hu, J. Kurths, and Z. Liu, Explosive synchronization in a general complex network, *Phys. Rev. E* **88**, 010802(R) (2013).
- [7] P. Ji, T. K. D. Peron, P. J. Menck, F. A. Rodrigues, and J. Kurths, Cluster Explosive Synchronization in Complex Networks, *Phys. Rev. Lett.* **110**, 218701 (2013).
- [8] I. Leyva, I. Sendiña-Nadal, J. A. Almendral, A. Navas, S. Olmi, and S. Boccaletti, Explosive synchronization in weighted complex networks, *Phys. Rev. E* **88**, 042808 (2013).
- [9] X. Zhang, Y. Zou, S. Boccaletti, and Z. Liu, Explosive synchronization as a process of explosive percolation in dynamical phase space, *Sci. Rep.* **4**, 5200 (2015).
- [10] Y. Zou, T. Pereira, M. Small, Z. Liu, and J. Kurths, Basin of Attraction Determines Hysteresis in Explosive Synchronization, *Phys. Rev. Lett.* **112**, 114102 (2014).
- [11] P. S. Skardal and A. Arenas, Disorder induces explosive synchronization, *Phys. Rev. E* **89**, 062811 (2014).
- [12] X. Zhang, S. Boccaletti, S. Guan, and Z. Liu, Explosive Synchronization in Adaptive and Multilayer Networks, *Phys. Rev. Lett.* **114**, 038701 (2015).
- [13] M. M. Danziger, O. I. Moskalenko, S. A. Kurkin, X. Zhang, S. Havlin, and S. Boccaletti, Explosive synchronization coexists with classical synchronization in the Kuramoto model, *Chaos* **26**, 065307 (2016).
- [14] P. Khanra, P. Kundu, C. Hens, and P. Pal, Explosive synchronization in phase-frustrated multiplex networks, *Phys. Rev. E* **98**, 052315 (2018).
- [15] A. Kumar, S. Jalan, and A. D. Kachhvah, Interlayer adaptation-induced explosive synchronization in multiplex networks, *Phys. Rev. Research* **2**, 023259 (2020).
- [16] P. Khanra, P. Kundu, P. Pal, P. Ji, and C. Hens, Amplification of explosive width in complex networks, *Chaos* **30**, 031101 (2020).
- [17] P. Khanra and P. Pal, Explosive synchronization in multilayer networks through partial adaptation, *Chaos, Solitons Fractals* **143**, 110621 (2021).
- [18] R. S. Pinto and A. Saa, Explosive synchronization with partial degree-frequency correlation, *Phys. Rev. E* **91**, 022818 (2015).
- [19] P. Kundu and P. Pal, Synchronization transition in Sakaguchi-Kuramoto model on complex networks with partial degree-frequency correlation, *Chaos* **29**, 013123 (2019).
- [20] C. Xu, Y. Sun, J. Gao, T. Qiu, Z. Zheng, and S. Guan, Synchronization of phase oscillators with frequency-weighted coupling, *Sci. Rep.* **6**, 21926 (2016).
- [21] S. Jalan, A. Kumar, and I. Leyva, Explosive synchronization in frequency displaced multiplex networks, *Chaos* **29**, 041102 (2019).
- [22] A. D. Kachhvah and S. Jalan, Delay regulated explosive synchronization in multiplex networks, *New J. Phys.* **21**, 015006 (2019).
- [23] T. K. D. Peron and F. A. Rodrigues, Explosive synchronization enhanced by time-delayed coupling, *Phys. Rev. E* **86**, 016102 (2012).
- [24] Z. G. Nicolaou, D. Eroglu, and A. E. Motter, Multifaceted Dynamics of Janus Oscillator Networks, *Phys. Rev. X* **9**, 011017 (2019).
- [25] H. Cao and Z. Liu, A novel synchronization transition and amplitude death in the local brain networks of cortical regions, *Nonlinear Dyn.* **108**, 2861 (2022).
- [26] T. Wu, X. Zhang, and Z. Liu, Understanding the mechanisms of brain functions from the angle of synchronization and complex network, *Front. Phys.* **17**, 31504 (2022).
- [27] S. Gupta, A. Campa, and S. Ruffo, Nonequilibrium first-order transition in coupled oscillator systems with inertia and noise, *Phys. Rev. E* **89**, 022123 (2014).
- [28] X. Li, X. Dai, D. Jia, H. Guo, S. Li, G. D. Cooper, K. Alfaro-Bittner, M. Perc, S. Boccaletti, and Z. Wang, Double explosive transitions to synchronization and cooperation in intertwined dynamics and evolutionary games, *New J. Phys.* **22**, 123026 (2020).
- [29] Y. Eom, S. Boccaletti, and G. Caldarelli, Concurrent enhancement of percolation and synchronization in adaptive networks, *Sci. Rep.* **6**, 27111 (2016).
- [30] C. Kuehn and C. Bick, A universal route to explosive phenomena, *Sci. Adv.* **7**, eabe3824 (2021).
- [31] The coexistence of two stable partially synchronized states was observed in the paper by O. E. Omel’chenko and M. Wolfrum [Nonuniversal Transitions to Synchrony in the Sakaguchi-Kuramoto Model, *Phys. Rev. Lett.* **109**, 164101 (2012)]. In that paper, it was found that two abrupt transitions can be expected, provided that a phase frustration with an appropriate choice for the frequency distribution is taken. However, in their paper, the order parameter of the first abrupt transition is even smaller than 0.5; that is, it is only a partially synchronized state. In this sense,

- the phenomenon observed cannot be considered as an explosive synchronization as defined in previous studies; see the review in Ref. [1] for details.
- [32] C. Tallon-Baudry, The roles of gamma-band oscillatory synchrony in human visual cognition, *Front. Biosci.* **14**, 321 (2009).
- [33] G. Deco, A. Buehlmann, T. Masquelier, and E. Hugues, The role of rhythmic neural synchronization in rest and task conditions, *Front. Hum. Neurosci.* **5**, 4 (2011).
- [34] P. Erdős and A. Rényi, On random graphs I, *Publ. Math. Debrecen* **6**, 290 (1959).
- [35] Y. Kuramoto, *Chemical Oscillations, Waves, and Turbulence* (Springer, New York, 1984); S. Strogatz, *Phys. D (Amsterdam)* **143**, 1 (2000).
- [36] The term “adiabatically” here means that, after each increment or decrement of $\delta\lambda$, a large time interval is allowed to elapse at the new value of λ (sufficient for the system to reach the asymptotic dynamics) before operating the next increment or decrement step.
- [37] See Supplemental Material at <http://link.aps.org/supplemental/10.1103/PhysRevResearch.4.033009> for a detailed theoretical description.
- [38] M. J. Panaggio and D. M. Abrams, Chimera states: coexistence of coherence and incoherence in networks of coupled oscillators, *Nonlinearity* **28**, R67 (2015).
- [39] J. M. Buldú and M. A. Porter, Frequency-based brain networks: From a multiplex framework to a full multilayer description, *Network Neurosci.* **2**, 418 (2018).
- [40] G. Buzsáki, *Rhythms of the Brain* (Oxford University Press, Oxford, 2006).
- [41] M. J. Brookes, P. K. Tewarie, B. A. E. Hunt, S. E. Robson, L. E. Gascoyne, E. B. Liddle, P. F. Liddle, and P. G. Morris, A multi-layer network approach to MEG connectivity analysis, *NeuroImage* **132**, 425 (2016).
- [42] M. Yu, M. M. A. Engels, A. Hillebrand, E. C. W. van Straaten, A. A. Gouw, C. Teunissen, W. M. van der Flier, P. Scheltens, and C. J. Stam, Selective impairment of hippocampus and posterior hub areas in Alzheimer disease: An MEG-based multiplex network study, *Brain* **140**, 1466 (2017).
- [43] L. Cocchi, L. L. Gollo, A. Zalesky, and M. Breakspear, Criticality in the brain: A synthesis of neurobiology, models and cognition, *Prog. Neurobiol.* **158**, 132 (2017).
- [44] M. Kim, G. A. Mashour, S.-B. Moraes, G. Vanini, V. Tarnal, E. Janke, A. G. Hudetz, and U. Lee, Functional and topological conditions for explosive synchronization develop in human brain networks with the onset of anesthetic-induced unconsciousness, *Front. Comput. Neurosci.* **10**, 1 (2016).
- [45] P. Hagmann, L. Cammoun, X. Gigandet, R. Meuli, C. J. Honey, J. V. Wedeen, and O. Sporns, Mapping the structural core of human cerebral cortex, *PLoS Biol.* **6**, e159 (2008).
- [46] C. J. Honey, O. Sporns, L. Cammoun, X. Gigandet, J. P. Thiran, R. Meuli, and P. Hagmann, Predicting human resting-state functional connectivity from structural connectivity, *Proc. Natl. Acad. Sci. USA* **106**, 2035 (2009).
- [47] K. Bansal, J. O. Garcia, S. H. Tompson, T. Verstynen, J. M. Vettel, and S. F. Muldoon, Cognitive chimera states in human brain networks, *Sci. Adv.* **5**, eaau8535 (2019).
- [48] S. V. Buldyrev, R. Parshani, G. Paul, H. E. Stanley, and S. Havlin, Catastrophic cascade of failures in interdependent networks, *Nature (London)* **464**, 1025 (2010).
- [49] M. Zheng, W. Wang, M. Tang, J. Zhou, S. Boccaletti, and Z. Liu, Multiple peaks patterns of epidemic spreading in multilayer networks, *Chaos, Solitons Fractals* **107**, 135 (2018).
- [50] H. Liu, M. Zheng, and Z. Liu, A paradox of epidemics between the state and parameter spaces, *Sci. Rep.* **8**, 7517 (2018).
- [51] M. Zheng, M. Zhao, B. Min, and Z. Liu, Synchronized and mixed outbreaks of coupled recurrent epidemics, *Sci. Rep.* **7**, 2424 (2017).
- [52] H. Liu, M. Zheng, D. Wu, Z. Wang, J. Liu, and Z. Liu, Hysteresis loop of nonperiodic outbreaks of recurrent epidemics, *Phys. Rev. E* **94**, 062318 (2016).